



HAL
open science

Pb isotope geochemistry of Piton de la Fournaise historical lavas

Ivan Vlastélic, Catherine Deniel, Chantal Bosq, Philippe Telouk, Pierre Boivin, Patrick Bachèlery, Vincent Famin, Thomas Staudacher

► **To cite this version:**

Ivan Vlastélic, Catherine Deniel, Chantal Bosq, Philippe Telouk, Pierre Boivin, et al.. Pb isotope geochemistry of Piton de la Fournaise historical lavas. *Journal of Volcanology and Geothermal Research*, 2009, 184, pp.63-78. 10.1016/j.jvolgeores.2008.08.008 . hal-00453654

HAL Id: hal-00453654

<https://hal.science/hal-00453654>

Submitted on 19 Nov 2021

HAL is a multi-disciplinary open access archive for the deposit and dissemination of scientific research documents, whether they are published or not. The documents may come from teaching and research institutions in France or abroad, or from public or private research centers.

L'archive ouverte pluridisciplinaire **HAL**, est destinée au dépôt et à la diffusion de documents scientifiques de niveau recherche, publiés ou non, émanant des établissements d'enseignement et de recherche français ou étrangers, des laboratoires publics ou privés.



Distributed under a Creative Commons Attribution - NonCommercial 4.0 International License

Pb isotope geochemistry of Piton de la Fournaise historical lavas

Ivan Vlastélic^{a,*}, Catherine Deniel^a, Chantal Bosq^a, Philippe Télouk^b, Pierre Boivin^a, Patrick Bachèlery^c, Vincent Famin^c, Thomas Staudacher^d

^a Laboratoire Magmas et Volcans, Observatoire de Physique du Globe de Clermont-Ferrand, Université Blaise Pascal, CNRS UMR 6524, 5 Rue Kessler, 63038 Clermont-Ferrand, France

^b Laboratoire des Sciences de la Terre, Ecole Normale Supérieure de Lyon, CNRS UMR 5570, 46 Allée d'Italie, 69364 Lyon cedex 07, France

^c Laboratoire GéoSciences Réunion, Université de La Réunion, Institut de Physique du Globe de Paris, CNRS UMR 7154, 15 Avenue René Cassin, 97715 Saint-Denis cedex 09, La Réunion, France

^d Observatoire Volcanologique du Piton de la Fournaise, Institut de Physique du Globe de Paris, CNRS UMR 7154, 14 RN3, le 27èmekm, 97418, La Plaine des Cafres, La Réunion, France

Variations of Pb isotopes in historical lavas (1927–2007) from Piton de la Fournaise are investigated based on new (116 samples) and published (127 samples) data. Lead isotopic signal exhibits smooth fluctuations ($18.87 < {}^{206}\text{Pb}/{}^{204}\text{Pb} < 18.94$) on which superimpose unradiogenic spikes (${}^{206}\text{Pb}/{}^{204}\text{Pb}$ down to 18.70). Lead isotopes are decoupled from ${}^{87}\text{Sr}/{}^{86}\text{Sr}$ and ${}^{143}\text{Nd}/{}^{144}\text{Nd}$, which display small and barely significant variations, respectively. No significant change of Pb isotope composition occurred during the longest (>3 years) periods of inactivity of the volcano (1939–1942, 1966–1972, 1992–1998), supporting previous inferences that Pb isotopic variations occur mostly during and not between eruptions. Intermediate compositions ($18.904 < {}^{206}\text{Pb}/{}^{204}\text{Pb} < 18.917$) bracket the longest periods of quiescence. In this respect, the highly frequent occurrence of an intermediate composition ($18.90 < {}^{206}\text{Pb}/{}^{204}\text{Pb} < 18.91$), which clearly defines an isotopic baseline during the most recent densely sampled period (1975–2007), either suggests direct sampling of plume melts or sampling of a voluminous magma reservoir that buffers Pb isotopic composition. Deviations from this prevalent composition occurred during well-defined time periods, namely 1977–1986 (radiogenic signature), 1986–1990 and 1998–2005 (unradiogenic signatures). The three periods display a progressive isotopic drift ending by a rapid return (mostly during a single eruption) to the isotopic baseline. The isotopic gradients could reflect progressive emptying of small magma reservoirs or magma conduits, which are expected to be more sensitive to wall-rock interactions than the main magma chamber. These gradients provide a lower bound ranging from 0.1 to 0.17 km³ for the size of the shallow magma storage system. The isotopic shifts (March 1986, January 1990 and February 2005) are interpreted as refilling the plumbing system with deep melts that have not interacted with crustal components. The volume of magma erupted between the two major refilling events of March 1986 and February 2005 (0.28 km³) could provide a realistic estimate of the magma reservoir size. Unradiogenic anomalies appear to be linked, more or less directly, to the eruption of olivine-rich lavas. The related samples have low ${}^{206}\text{Pb}/{}^{204}\text{Pb}$ and ${}^{208}\text{Pb}/{}^{204}\text{Pb}$ but normal ${}^{207}\text{Pb}/{}^{204}\text{Pb}$, suggesting a recent decrease of U/Pb and Th/Pb, for instance through sequestration of Pb into sulfides. Olivine and sulfides, which are both denser than silicate melts, could be entrained with magma pulses, which give rise to high-flux oceanite eruptions.

1. Introduction

By comparison to hotspot volcanism worldwide, Réunion volcanoes produce lavas with remarkably uniform Sr, Nd and He isotopic compositions (Fisk et al., 1988; Graham et al., 1990; Staudacher et al., 1990; Albarède et al., 1997; Fretzdorff and Haase, 2002). Even the subtle temporal increase of ${}^{143}\text{Nd}/{}^{144}\text{Nd}$ identified at Piton de la Fournaise (Luais, 2004) has recently been questioned (Bosch et al., 2008). On the other hand, it has been early recognized (Oversby, 1972) that Pb isotopic composition is more variable. Piton des Neiges and Piton de la Fournaise lavas exhibit distinct Pb isotope signatures, and

both volcanoes display a temporal trend toward less radiogenic compositions (Bosch et al., 2008). According to Bosch et al. (2008), these Pb isotopic variations may reflect progressive melting of two ascending blobs of different composition within the plume conduit. Temporal variations of Pb isotopes have also been identified in very recent lavas (1998–2006) erupted at Piton de la Fournaise. However, at such a short time-scale, the isotopic variations may dominantly reflect interaction of plume magmas with wall-rocks, including preexisting lava flows building the edifice and genetically unrelated rocks of the underlying oceanic basement (Vlastélic et al., 2005). If this interpretation is correct, short-term fluctuations of Pb isotopes could be used to distinguish periods of emptying the magma storage system from those of refilling the plumbing system with deep melts that have not interacted with crustal components. Albarède (1993) introduced the

* Corresponding author. Tel.: +33 4 73 34 67 10; fax: +33 4 73 34 67 44.
E-mail address: I.Vlastelic@opgc.univ-bpclermont.fr (I. Vlastélic).

idea that fast changes in isotopic and incompatible element ratios in volcanic series provide strong constraints on magma reservoir dynamics. Following this idea, the most recent Pb isotopic evolution of Piton de la Fournaise lavas has been used to discuss the size and shape of the magma storage system (Vlastélic et al., 2007).

This paper investigates the variations of Pb isotopes of Piton de la Fournaise lavas at the century scale (1927–2007), with the aim of better constraining the cycles of magma supply and storage. We analyzed 116 new samples with special emphasis on the 1953–1992 period and the most recent eruptions (2006–2007), including the voluminous eruption of April 2007. These data, together with previously published data from the 1998–2006 period (Vlastélic et al., 2005, 2007) form an extensive data set of 230 Pb isotopic analyses. We also report the Pb isotopic composition of three old samples recovered from the Grand Brûlé drill hole, which compositions are used to evaluate the extent to which lavas interact with the deep layers of the edifice. In addition, a subset of samples has been analyzed for Sr and Nd isotopes in order to better understand the meaning of the Pb isotopic signal.

2. Geological and geochemical background

About 1 km³ of lava has been erupted from 1920 to 2007 (Fig. 1). The most voluminous eruptions occurred in 1931 (130 Mm³), 2007 (120 Mm³), 1961 (60 Mm³) and 1998 (60 Mm³), the two first causing major collapses within the Dolomieu crater (Bachèlery, 1981; Michon et al., 2007; Staudacher et al., 2009–this issue). The rate of magma production seems to have increased during the 20th century and is

particularly high (>0.6 m³/s) since 1998. The apparent low productivity before 1961 could reflect a less detailed observation of volcanic activity, however. Long periods of inactivity (>3 years) occurred in 1966–1972 and 1992–1998, and also probably in 1934–1937 and 1939–1942. All eruptions occurred inside the enclos Fouqué caldera, with the exception of March 1977 and March 1998 eruptions, which propagated along the NE rift zone, and March 1986 eruption, which propagated along the SE rift zone (see Fig. 2 and Vlastélic et al., 2005, 2007).

Historical lavas from Piton de la Fournaise mainly consist of cotectic basalts (clinopyroxene–olivine–plagioclase phyrlic basalts) and oceanites (olivine-rich basalts with MgO>20 wt.%). Oceanite eruptions occurred regularly (1927, 1931, 1938, 1948, 1953, 1961, 1977, 2002, 2005, 2006 and 2007) and account for most of MgO variations (Fig. 1). By comparison, olivine-rich basalt with 10<MgO<20 wt.% occurred much more rarely (1945, 1972), with the exception of recent, densely sampled eruptions (in particular between 2001 and 2007), possibly reflecting a sampling bias. Olivine fractionation accounts for small MgO variations (typically between 6 and 9%). CaO/Al₂O₃, which is thought to dominantly record clinopyroxene removal, varies over ~17 years cycles and generally negatively correlates with incompatible element enrichment (Albarède and Tamagnan, 1988). Oceanites and olivine-rich lavas are often depleted in light rare earth elements (i.e. low Ce/Yb or La/Sm ratios) compared to contemporaneous cotectic basalts (Albarède and Tamagnan, 1988; Vlastélic et al., 2007). Sr and Nd isotopic compositions display small variations (0.70407<⁸⁷Sr/⁸⁶Sr<0.70425; +3.9<ε_{Nd}<+4.3) but Pb isotopes are more variable (18.76<²⁰⁶Pb/²⁰⁴Pb<18.95) (Albarède and Tamagnan, 1988; Albarède et al., 1997; Vlastélic et al., 2005, 2007; Bosch et al., 2008).

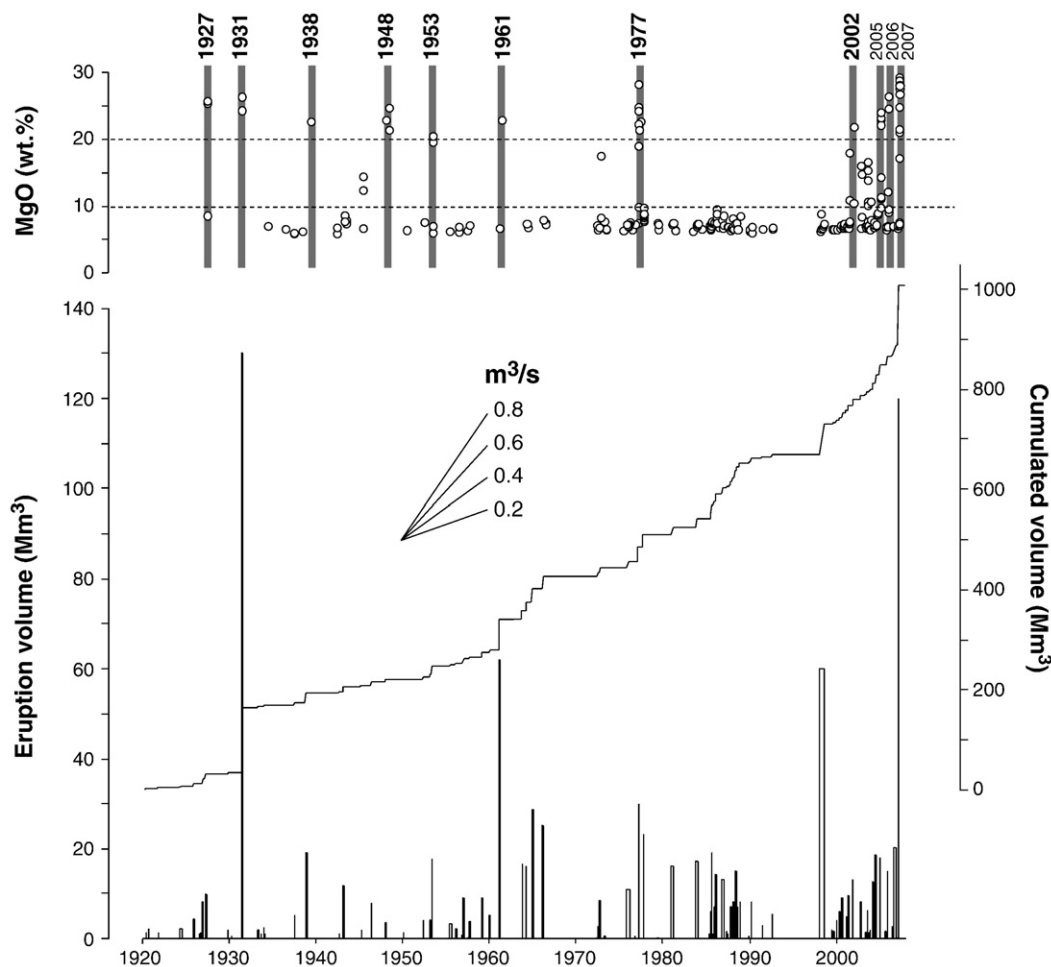


Fig. 1. Eruption volumes and cumulated volume of lava erupted since 1927. Data sources: Bachèlery (1981), Stieltjes and Moutou (1989), Lénat et al. (1989), Vlastélic et al. (2005, 2007) and unpublished data. Note that the volume of April 1977 eruption is probably much lower than previously estimated (J.F. Lénat, personal communication, 2008). High magnesium content (MgO>20 wt.%, vertical grey bands) reflects the occurrence of olivine-rich lavas and oceanites.

3. Samples selection for Pb, Sr and Nd isotopes analysis

One hundred sixteen new samples were selected for Pb isotope analysis, including 63 samples from the 1977–1992 period (Boivin and Bachèlery, 2009–this issue), 15 samples erupted between 1957 and 1976 (Bachèlery, 1981), 9 samples from the 1927–1977 period (Albarède et al., 1997), and 29 samples from the most recent activity (2006–2007) (sixteen of which being from the unusually productive eruption of April 2007, Staudacher et al., 2009–this issue). Three samples erupted on the 2nd of July 2001 and having anomalously unradiogenic Pb composition (Vlastélic et al., 2005) have been re-analyzed. We also report the Pb isotopic composition of three samples of gabbroic cumulates recovered between 1827 m and 2442 m within the Grand Brûlé drill hole (Fig. 2) (Rançon et al., 1989). These samples would belong to the shallow magma chamber of an ancient volcano that was active >0.78 Ma ago (Lénat and Gibert-Malengreau, 2001). Seventeen samples covering the whole range of Pb isotopic variations have been selected for Sr and Nd isotopes analysis.

4. Analytical techniques

4.1. Pb isotopic compositions

Millimeter-sized rock chips (about 200 mg) were leached with 0.5 N HCl for 1 h at room temperature and subsequently dissolved in a

mixture of concentrated HF (3 ml) and HNO₃ (1 ml) for 24 h at 80 °C. Fluorides were eliminated by taking up samples successively in concentrated HNO₃ (1 ml) and 6 N HCl (1 ml). Lead converted to bromide form was extracted (first pass) and purified (second pass) on 30 µl teflon columns filled with strong anion exchange resin (Bio-Rad AG1-X8 100–200 mesh) using HNO₃–HBr mixtures (Lugmair and Galer, 1992). The procedural blanks (<50 pg) are negligible compared to the amount of lead purified (>200 ng). Organic material and Br left after chemical separation were eliminated with a few drops of concentrated HNO₃. The amount of Pb extracted was estimated at this stage by analyzing an aliquot of the solutions by quadrupole ICPMS (Laboratoire Magmas et Volcans, Clermont-Ferrand). After optimal dilution (40 ppb Pb solutions), isotopic compositions were measured automatically by MC-ICPMS (Nu instrument 041, Ecole Normale Supérieure de Lyon) using a Tl spike to monitor instrumental mass fractionation (White et al., 2000). Samples were introduced through a desolvator (Nu DSN) at a rate of 100 µl/min, yielding a total Pb beam of ca. 10 V for 40 ppb Pb solutions. The NBS 981 standard measured every two samples revealed the absence of instrumental drift during the typically 24 hours sessions. The external precision was thus inferred from repeated analysis of the NBS 981 standard (2σ error of 170, 160, 150, 60 and 40 ppm for ²⁰⁸Pb/²⁰⁴Pb, ²⁰⁷Pb/²⁰⁴Pb, ²⁰⁶Pb/²⁰⁴Pb, ²⁰⁸Pb/²⁰⁶Pb and ²⁰⁷Pb/²⁰⁶Pb ratios, respectively). These precisions are two to six times better than those previously obtained on the first generation MC-ICPMS VG P54 (Vlastélic et al., 2005).

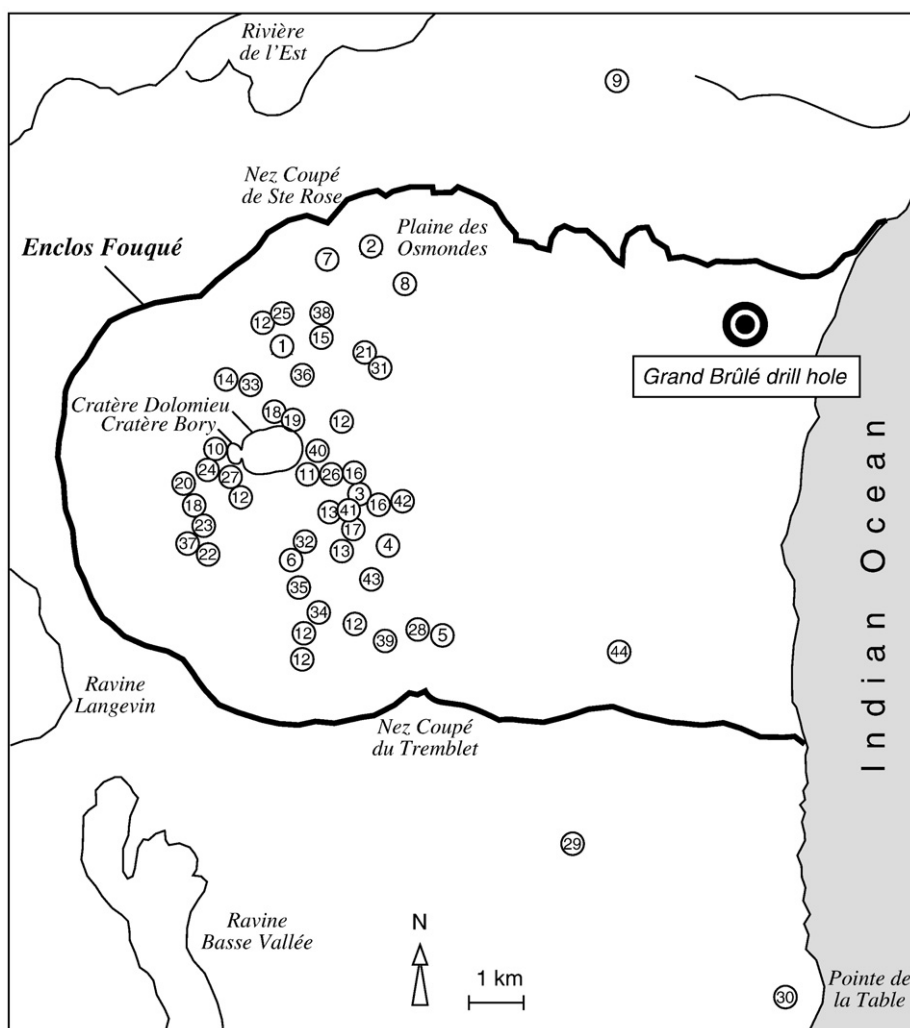


Fig. 2. Map of Piton de la Fournaise volcano showing the locations of eruption vents. Numbers refer to the vents listed in Table 1. Note that vent locations and eruption dates are less precisely known for samples erupted before 1977. The location of the Grand Brûlé drill hole, 172 m above sea level, is also indicated (Rançon et al., 1989).

Table 1

Pb isotopic compositions.

Eruption	Sample name	Eruption date	Vents Location	²⁰⁶ Pb/ ²⁰⁴ Pb	²⁰⁷ Pb/ ²⁰⁴ Pb	²⁰⁸ Pb/ ²⁰⁴ Pb
January 1927	T2101	1927/01–1927/02	1	18.8917	15.5866	38.9843
	T2101 dup			18.9001	15.5899	38.9875
January 1931	T1602	1931/01–1931/08	2	18.8970	15.5879	38.9833
	T1602 dup			18.8929	15.5864	38.9700
December 1938	P1601	1938/12–1939/01	3	18.9106	15.5924	38.9960
April 1943	N2201	1943/04–1943/05	4	18.9118	15.5910	38.9951
April 1945	PF1945	1945/04–1945/05	5	18.9103	15.5932	38.9960
February 1948	O1401	1948/02	6	18.8904	15.5876	38.9727
June 1953	T1904	1953/06–1953/07	7	18.8958	15.5897	38.9848
April 1961	GB1961	1961/04	8	18.9069	15.5941	39.0027
March 1977	SR1977	1977/03–1977-04	9	18.9337	15.5965	39.0344
	SR1977 dup			18.9311	15.5980	39.0319
	SR1977 ter			18.9258	15.5973	39.0265
September 1957	80–99	1957/09–1957/11	10	18.9013	15.5927	38.9988
March 1966	80–91	1966/03–1966/05	11	18.9173	15.5951	39.0198
June 1972	80–89	1972/06	12	18.9164	15.5959	39.0204
October 1972	1972–12	1972/11	12	18.9126	15.5976	39.0192
	1972–13	1972/12	12	18.9081	15.5954	39.0178
May 1973	80–76	1973/05	D	18.9100	15.5950	39.0168
November 1975	80–75	1975/11	D	18.9061	15.5946	39.0105
December 1975	10S11	1975/12/18	13	18.9103	15.5953	39.0186
	9S11b	1975/12–1976/01	13	18.9114	15.5959	39.0165
	6S11	1975/12–1976/01	13	18.9110	15.5961	39.0172
	1X9	1976/01	13	18.9109	15.5950	39.0154
	8V9a	1976/01	13	18.9098	15.5947	39.0138
	7W10	1976/01–1976/03	13	18.9108	15.5934	39.0129
	6T11F	1976/03–1976-04	13	18.9156	15.5973	39.0259
November 1976	5R12	1976/11	14	18.9208	15.5973	39.0285
24 March 1977	RU 77-3	1977/4/1	15	18.9217	15.5959	39.0238
	RU 77-7	1977/4/8	9	18.9346	15.5980	39.0375
24 October 1977	RU 77-11	1977/10/24	16	18.8709	15.5968	38.9627
	RU 77-11 dup			18.9314	15.5988	39.0360
	RU 77-11 ter			18.9174	15.5973	39.0183
	RU 77-13	1977/10/31	16	18.9184	15.5982	39.0202
	RU 77-14	1977/11/4	16	18.6972	15.5923	38.7717
	RU 77-14 dup			18.8611	15.5942	38.9530
	RU 77-14 ter			18.8944	15.5977	38.9945
	RU 77-16	1977/11/7	16	18.9231	15.5972	39.0241
	RU 77-17	1977/11/11	16	18.9133	15.5955	39.0091
RU 77-18	1977/11/13	16	18.9343	15.5992	39.0361	
28 May 1979	795-23	1979/5/28	17	18.9316	15.5973	39.0290
13 July 1979	JUIL 79 M	1979/7/13	18	18.9184	15.5960	39.0155
3 February 1981	8102-16	1981/2/16	19	18.9335	15.6022	39.0427
	813-1	1981/3/1	20	18.9355	15.5989	39.0343
	814-1	1981/4/1	21	18.9343	15.5993	39.0339
4 December 1983	83-409	1983/12/4	22	18.9352	15.5981	39.0362
	83-409 dup	1983/12/4	22	18.9369	15.5973	39.0343
	83-63	1983/12/6	22	18.9395	15.5993	39.0394
	83-210	1983/12/21	22	18.9387	15.5984	39.0353
	83-290	1983/12/29	22	18.9402	15.6002	39.0419
18 January 1984	841-240	1984/1/24	23	18.9350	15.5988	39.0324
	841-272	1984/1/27	23	18.9398	15.5987	39.0378
	842-75	1984/2/7	23	18.9425	15.6015	39.0480

Table 1 (continued)

Eruption	Sample name	Eruption date	Vents Location	$^{206}\text{Pb}/^{204}\text{Pb}$	$^{207}\text{Pb}/^{204}\text{Pb}$	$^{208}\text{Pb}/^{204}\text{Pb}$
14 June 1985	856-141	1985/6/14	24	18.9423	15.6008	39.0447
5 August 1985	858-73	1985/8/7	25	18.9426	15.5995	39.0407
	858-142	1985/8/14	25	18.9427	15.5994	39.0399
	858-281	1985/8/28	25	18.9437	15.6009	39.0448
6 September 1985	859-61	1985/9/6	26	18.9385	15.5989	39.0348
	859-161	1985/9/16	26	18.9355	15.5981	39.0326
	859-261	1985/9/26	26	18.9396	15.5979	39.0342
	859-301	1985/9/30	26	18.9368	15.5992	39.0354
2 December 1985	8512-23	1985/12/2	27	18.9387	15.5983	39.0357
29 December 1985	861-62	1986/1/6	D	18.9378	15.5984	39.0331
	861-173	1986/1/17	D	18.9369	15.5978	39.0311
19 March 1986	863-191	1986/3/19	28	18.9298	15.5981	39.0238
	863-204	1986/3/20	29	18.9301	15.5986	39.0253
	863-221	1986/3/22	29	18.9309	15.5989	39.0244
	863-242	1986/3/24	30	18.9250	15.5985	39.0160
	863-251	1986/3/25	30	18.9255	15.5975	39.0163
	863-281	1986/3/28	30	18.9178	15.5963	39.0048
	864-A101	1986/3/30	30	18.9277	15.5998	39.0239
	864-A113	1986/3/30	D	18.9374	15.5985	39.0329
12 November 1986	8611-12	1986/11/12	D	18.9138	15.5964	39.0047
26 November 1986	8611-26	1986/11/26	D	18.9108	15.5962	39.0012
6 December 1986	8612-71	1986/12/7	D	18.9120	15.5956	39.0017
	8612-152	1986/12/15	D	18.9131	15.5971	39.0053
6 December 1986	871-82	1987/1/6	31	18.9108	15.5956	38.9986
	871-170	1987/1/17	31	18.9074	15.5948	38.9939
10 June 1987	876-152	1987/6/15	D	18.9099	15.5954	38.9972
19 July 1987	877-191	1987/7/19	32	18.9043	15.5959	38.9976
6 November 1987	8711-61	1987/11/6	33	18.9030	15.5954	38.9955
30 November 1987	8712-51	1987/12/5	34	18.8986	15.5938	38.9907
	8712-221	1987/12/22	34	18.8985	15.5945	38.9905
7 February 1988	882-90	1988/2/9	35	18.8979	15.5952	38.9950
	882-140	1988/2/14	35	18.8988	15.5978	39.0042
	883-250	1988/3/25	35	18.8964	15.5940	38.9886
18 May 1988	885-1	1988/5/18	36	18.8937	15.5942	38.9881
	887-1	1988/7/1	36	18.8931	15.5943	38.9875
31 August 1988	888-311	1988/8/31	37	18.8896	15.5930	38.9818
14 December 1988	8812-181	1988/12/18	38	18.8932	15.5921	38.9841
18 January 1990	901-18	1990/1/18	D	18.9141	15.5950	39.0082
18 April 1990	904-18	1990/4/18	39	18.8794	15.5932	38.9606
	904-19	1990/4/19	39	18.8897	15.5936	38.9803
19 July 1991	917-191	1991/7/19	D + 40	18.9030	15.5956	38.9977
27 August 1992	928-27	1992/8/27	D + 41	18.8999	15.5942	38.9901
	928-28	1992/8/28	D + 41	18.9042	15.5943	38.9968
June 2001	010702-2	2001/7/2	42	18.8842	15.5921	38.9806
	010702-2 q	2001/7/2	42	18.8863	15.5927	38.9841
	010702-1	2001/7/2	42	18.8817	15.5918	38.9764
30 August 2006	0608-302	2006/8/30	D	18.9051	15.5946	39.0041
	0608-311	2006/8/31	D	18.9007	15.5906	38.9941
	0609-131	2006/9/13	D	18.9030	15.5918	38.9980
	0609-281	2006/9/28	D	18.9030	15.5924	38.9986
	0610-111	2006/10/11	D	18.9037	15.5934	38.9999
	0610-261	2006/10/26	D	18.9031	15.5949	39.0059
	0610-311	2006/10/31	D	18.9036	15.5933	39.0002
	0611-142	2006/11/14	D	18.8998	15.5894	38.9891
	0612-111	2006/12/11	D	18.9027	15.5932	38.9996

(continued on next page)

Table 1 (continued)

Eruption	Sample name	Eruption date	Vents Location	$^{206}\text{Pb}/^{204}\text{Pb}$	$^{207}\text{Pb}/^{204}\text{Pb}$	$^{208}\text{Pb}/^{204}\text{Pb}$
30 August 2006	0612-191	2006/12/19	D	18.9000	15.5895	38.9909
	0612-281	2006/12/28	D	18.9016	15.5915	38.9931
18 February 2007	0702-18-2	2007/2/18	D	18.9054	15.5950	39.0031
	0702-18-3	2007/2/18	40	18.9042	15.5935	39.0008
30 March 2007	070331-1	2007/3/30	43	18.9038	15.5930	38.9981
2 April 2007	070402-1	2007/4/2	44	18.9046	15.5935	39.0003
	070403-	2007/4/3	44	18.9025	15.5917	38.9946
	070404-	2007/4/4	44	18.9030	15.5944	38.9998
	070405-1	2007/4/5	44	18.8356	15.5843	38.9149
	070405-2	2007/4/5	44	18.9087	15.5922	38.9936
	070406-	2007/4/6	44	18.9079	15.5934	38.9947
	070406-1	2007/4/6	44	18.9110	15.5930	38.9977
	070407-1	2007/4/7	44	18.9064	15.5928	38.9969
	070408-1	2007/4/8	44	18.9074	15.5932	39.0005
	070417-1	2007/4/17	44	18.9090	15.5953	39.0074
	070420-2	2007/4/20	44	18.9017	15.5918	38.9898
	070420-2 dup			18.9030	15.5899	38.9871
	070425-1	2007/4/25	44	18.9059	15.5922	38.9944
	070425-2	2007/4/25	44	18.9069	15.5934	38.9997
	070425-2 dup			18.9067	15.5923	38.9955
	070428-1	2007/4/27	44	18.9076	15.5946	39.0028
	070429-1	2007/4/29	44	18.9083	15.5936	38.9994
	070429-1 dup			18.9083	15.5934	38.9999
			Depth (m)			
Grand Brûlé Drill Hole	K3-1	>0.78 Ma	1827	18.9650	15.5979	39.0481
	K3-2	>0.78 Ma	1827	18.9544	15.5969	39.0267
	K5C1	>0.78 Ma	2442	18.9313	15.6029	39.0239

Pb isotopic compositions are relative to NBS 981 values:

$^{206}\text{Pb}/^{204}\text{Pb} = 16.9356$, $^{207}\text{Pb}/^{204}\text{Pb} = 15.4891$, $^{208}\text{Pb}/^{204}\text{Pb} = 36.7006$.

dup: duplicate dissolution; ter: triplicate dissolution.

See Fig. 2 for vents locations.

Samples references:

1927–1977 samples: Albarède and Tamagnan (1988), Albarède et al. (1997), Sigmarsson et al. (2005).

1957–1976 samples: Bachèlery (1981).

1977–1992 samples: Boivin and Bachèlery (2009–this issue).

July 2001 samples: Vlastélic et al. (2005).

2006–2007 samples: new samples.

Grand Brûlé drill hole samples: Rançon et al. (1989).

4.2. Sr and Nd isotopic compositions

About 100 mg of either powder or rock chips were digested with mixed HF–HNO₃–HClO₄ acids. Three dried sample fractions arising from Pb chemistry were redissolved in 1 ml 6 M HCl plus 1 ml 10 M HNO₃. After drying, all the samples were taken up in 6 M HCl, warmed, and evaporated before final dissolution in 1.25 M HCl. Iron (and titanium) were mostly removed from the samples using a strong cation exchanger (Bio-Rad AG50-X4, 200–400 mesh) (Pin and Zalduégui, 1997). A tandem column elution scheme using the Sr.Spec and Tru.Spec chromatographic materials was then used to achieve the concomitant separation of Sr and LREE (Pin et al., 1994). Nd was then purified from the adjacent lanthanides, especially Sm, using the Ln.Spec chromatographic material (Pin and Zalduégui, 1997). The measurements were performed on a nine collectors Triton mass spectrometer, either in a static or dynamic mode. $^{87}\text{Sr}/^{86}\text{Sr}$ and $^{143}\text{Nd}/^{144}\text{Nd}$ ratios were normalized to $^{86}\text{Sr}/^{88}\text{Sr} = 0.1194$ and $^{146}\text{Nd}/^{144}\text{Nd} = 0.7219$, respectively. Sr and Nd isotopic ratios are given relative to $^{87}\text{Sr}/^{86}\text{Sr} = 0.710243 \pm 9$ (2 SD, 20 measurements) for NBS SRM 987 and $^{143}\text{Nd}/^{144}\text{Nd} = 0.511958 \pm 8$ (2 SD, 16 measurements) for Ames Rennes. Analytical blanks were about 1 ng for both Sr and Nd isotope measurements.

5. Results

5.1. Pb isotopes distribution

Data reported in Table 1 together with previously published data from the 1998–2006 period (Vlastélic et al., 2005, 2007) reveal a

bimodal distribution of Pb isotopes in Piton de la Fournaise historical lavas (Fig. 3). The dominant peak of $^{206}\text{Pb}/^{204}\text{Pb}$, which includes 200 analyses, ranges from 18.865 to 18.920. Within this group, isotopic compositions varying between 18.900 and 18.905 are by far the most frequent (38 analyses). The second peak is made of 40 more radiogenic compositions ($18.920 < ^{206}\text{Pb}/^{204}\text{Pb} < 18.945$). Eight unradiogenic compositions ($^{206}\text{Pb}/^{204}\text{Pb} \leq 18.865$) do not belong to these two groups, and are therefore referred to as “anomalous compositions”. Note that these anomalous compositions have no radiogenic counterparts. By comparison, Pb isotope compositions of lavas produced since 527 ky (Fig. 3) extent to more radiogenic compositions ($^{206}\text{Pb}/^{204}\text{Pb}$ up to 19.012), which are generally found in the oldest lavas (Bosch et al., 2008).

5.2. Pb isotopes versus time

Plotting Pb isotopes versus time (Fig. 4) reveals the following main features: (1) Lead isotopic compositions do not define a secular trend but, instead, display smooth and generally fast fluctuations (typically decennial to monthly) around a prevalent composition ($^{206}\text{Pb}/^{204}\text{Pb} = 18.90$; $^{208}\text{Pb}/^{204}\text{Pb} = 39.0$; $^{208}\text{Pb}/^{206}\text{Pb} = 2.063$; $^{207}\text{Pb}/^{206}\text{Pb} = 0.825$). (2) Major departures from this composition occur during well-defined time intervals, namely 1977–1986 (radiogenic signature) and 1999–2005 (unradiogenic signature). (3) In contrast to Pb/Pb ratios, $(^{208}\text{Pb})^*/(^{206}\text{Pb})^*$ (the radiogenic $^{208}\text{Pb}/^{206}\text{Pb}$ ratio, which is defined in Fig. 4 caption) is rather constant. (4) Rare, but pronounced unradiogenic anomalies ($^{206}\text{Pb}/^{204}\text{Pb}$ down to 18.697) are identified in recent, densely sampled eruptions (October 1977, July 2001, August 2003, February 2005 and April 2007). These isotopic spikes seem to be linked to eruption of olivine-rich lavas

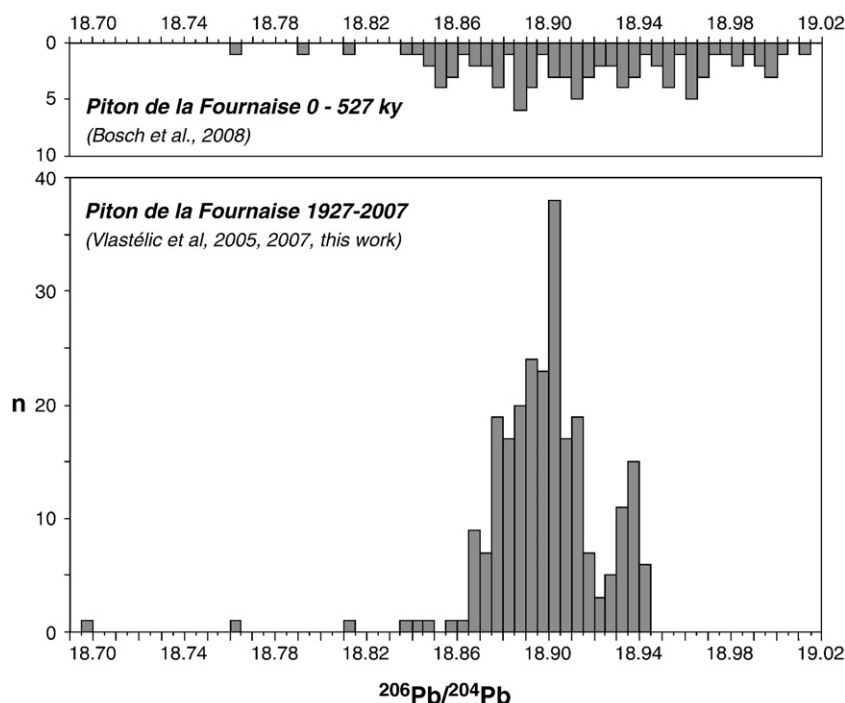


Fig. 3. Distribution of $^{206}\text{Pb}/^{204}\text{Pb}$ in historical lavas from Piton de la Fournaise (data from Table 1 and Vlastélic et al., 2005, 2007). By comparison, the distribution of $^{206}\text{Pb}/^{204}\text{Pb}$ in samples covering 527 ky of volcanic activity is also shown (data from Bosch et al., 2008).

(Fig. 5). Close inspection of the related eruptions suggests that the isotopic anomalies generally coincide with transitions from basalts to oceanites. In October 1977, an anomalous composition occurred a few months after the oceanite eruption (March 1977), but nevertheless coincided with eruption of olivine-bearing basalts (MgO up to 9.70 wt.%). (5) Isotopic variations occur mostly during eruptions and not between. For instance, the Pb isotopic composition of the first magma erupted in March 1998 is very similar to that of the last lavas of the preceding eruption, which occurred nearly six years earlier (August 1992). On the other hand, large isotopic variations are observed during relatively short eruptions (such as March 1986 or February 2005). As previously suggested (Vlastélic et al., 2007), plotting Pb isotope compositions against cumulated days of eruption (i.e. removing periods of quiescence) reveals the fine features of isotopic variations. Such plot requires a good knowledge of both eruptions and sampling chronology, and is thus only shown for the most recent eruptions (1975–2007) (Fig. 6). Three distinct time periods can be distinguished on the basis of lead isotope temporal trends: 1975–1985 (positive $^{206}\text{Pb}/^{204}\text{Pb}$ gradient), 1986–1990 and 1998–2004 (negative $^{206}\text{Pb}/^{204}\text{Pb}$ gradients). The three periods ended by rapid returns to the isotopic baseline. In 1986 and 2005, abrupt isotopic shifts occurred mainly during single eruptions, namely March 1986 and February 2005 eruptions, respectively. The isotopic shift of 1990 is of lower magnitude and is temporally less well-defined. Note that the gradients systematically diverge from the baseline, whereas the isotopic shifts systematically converge towards it (Fig. 6).

5.3. Sample heterogeneity

Replicate analyses indicate that normal compositions are reproducible whereas anomalous compositions are not necessarily (Table 1). This suggests that the samples having anomalous Pb isotope compositions are heterogeneous at the millimeter scale. For instance $^{206}\text{Pb}/^{204}\text{Pb}$ varies between 18.6972 and 18.8944 in sample RU77-14 (October 1977 eruption) showing, in turn, the least radiogenic composition measured in Piton de la Fournaise lavas. Duplicate analyses of the samples erupted the 2nd of July 2001 do not reproduce the anomalous compositions previously reported ($^{206}\text{Pb}/^{204}\text{Pb}$ down to

18.763 (Vlastélic et al., 2005)), but, instead, yield compositions which are both uniform ($^{206}\text{Pb}/^{204}\text{Pb}$ from 18.8817 to 18.8863) and similar to those of other samples from this eruption (Fig. 5). This lack of reproducibility could be the result of different leaching procedures: a stronger leaching was performed in our previous study (6 M HCl against 0.5 M HCl in this work). However, as the weakly leached samples display normal isotope compositions, removal of contaminated Pb by leaching cannot account for the observed discrepancy. It is thus concluded that samples from the 2nd of July 2001 consist of an unradiogenic phase resistant to HCl and a more soluble radiogenic phase (see discussion).

5.4. Pb–Pb isotope relationships

Lead–lead isotope relationships are illustrated in Fig. 7 using ^{204}Pb as the normalizing isotope. In $^{208}\text{Pb}/^{204}\text{Pb}$ versus $^{206}\text{Pb}/^{204}\text{Pb}$ space, historical samples, including those with anomalous compositions, plot along a single linear array passing through the composition of the primitive earth. The new, highly precise Nu MC-ICPMS data resolve, for the first time at such a short time-scale, change in $^{207}\text{Pb}/^{204}\text{Pb}$, and allow inspection of the relationship between $^{207}\text{Pb}/^{204}\text{Pb}$ and $^{206}\text{Pb}/^{204}\text{Pb}$. The anomalous samples, and in particular those from October 1977 and June 2001 eruptions plot off the array defined by normal samples, with anomalously low $^{206}\text{Pb}/^{204}\text{Pb}$ (and $^{208}\text{Pb}/^{204}\text{Pb}$), but normal $^{207}\text{Pb}/^{204}\text{Pb}$. If interpreted as a secondary isochron, the main array yields an age of 2.43 Ga. Taking this age as that of U/Pb increase, the Pb isotopic variations can be modeled in a two-stage μ history, with $\mu_1 = 7.93$ and μ_2 ranging from 10.95 to 11.20. In Pb–Pb isotopic space, the old cumulates from the Grand Brûlé drill hole plot near the radiogenic end of the isotopic array defined by historical samples, which is consistent with the observation that early products of Piton de la Fournaise had relatively radiogenic Pb compositions (Bosch et al., 2008).

5.5. Sr and Nd versus Pb isotope compositions

Sr and Nd isotopic compositions (Table 2) of a sample subset covering the whole range of Pb isotopic variations (Vlastélic et al.,

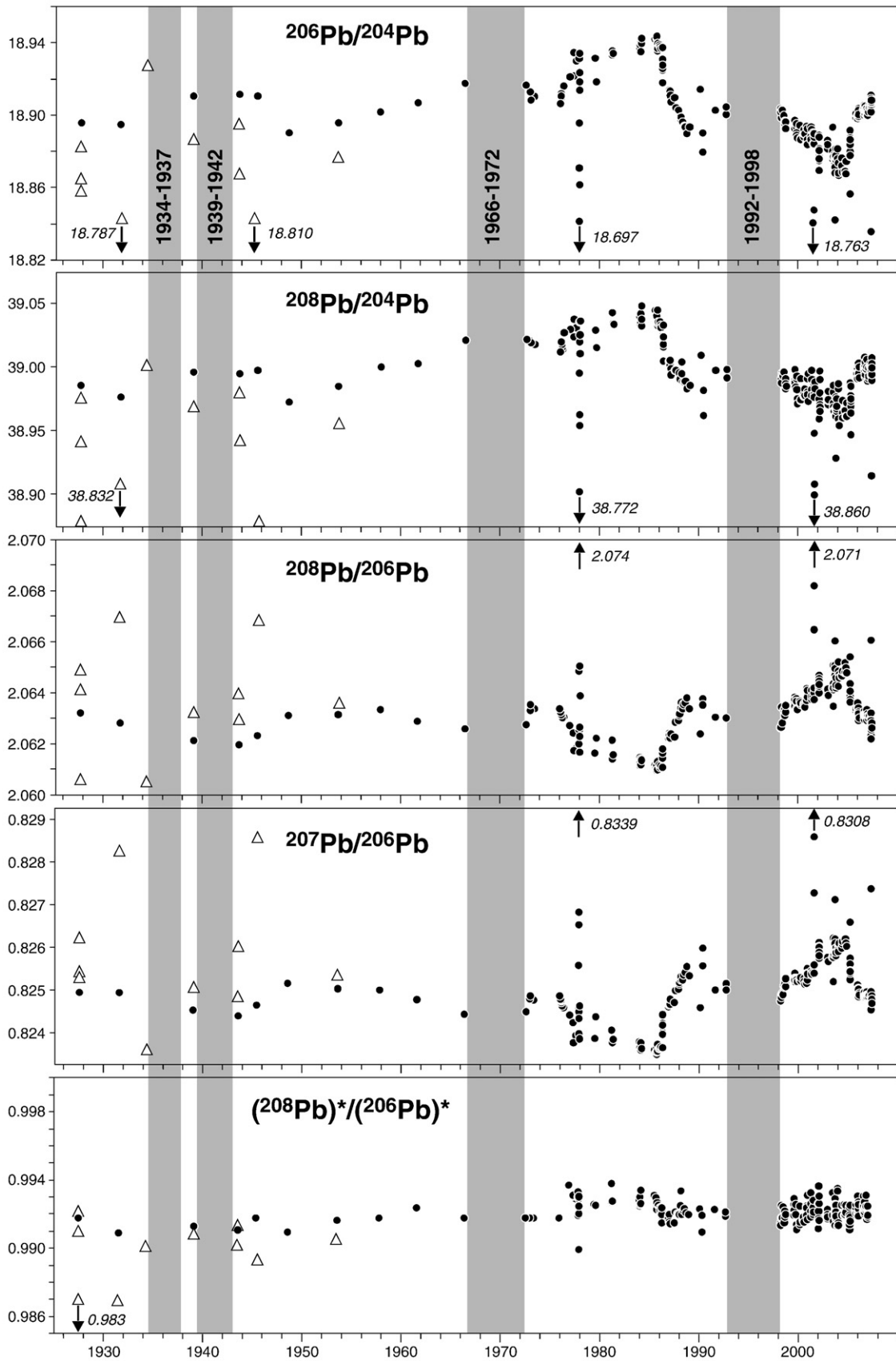


Fig. 4. Variation of Pb isotopes in Piton de la Fourmaise lavas erupted between 1927 and 2007. Data (closed circles) are from Table 1 and Vlastélic et al. (2005, 2007). Bosch et al. (2008) data, which have been re-normalized to the NBS 981 values reported in Table 1, are also shown using a distinctive symbol (triangles). Arrows point to out of scale compositions. All data were acquired on a Nu MC-ICPMS with the exception of Vlastélic et al. (2005) and Bosch et al. (2008) data, which were acquired on a VG P54 MC-ICPMS. Vertical grey bands indicate the longest periods of inactivity (>3 years). $(^{208}\text{Pb})^*/(^{206}\text{Pb})^*$ is the ratio of radiogenic ^{208}Pb over radiogenic ^{206}Pb : $(^{208}\text{Pb})^*/(^{206}\text{Pb})^* = [(^{208}\text{Pb}/^{204}\text{Pb})_S - (^{208}\text{Pb}/^{204}\text{Pb})_{\text{CD}}] / [(^{206}\text{Pb}/^{204}\text{Pb})_S - (^{206}\text{Pb}/^{204}\text{Pb})_{\text{CD}}]$ with subscripts S and CD referring to sample and Canyon Diablo meteorite, respectively.

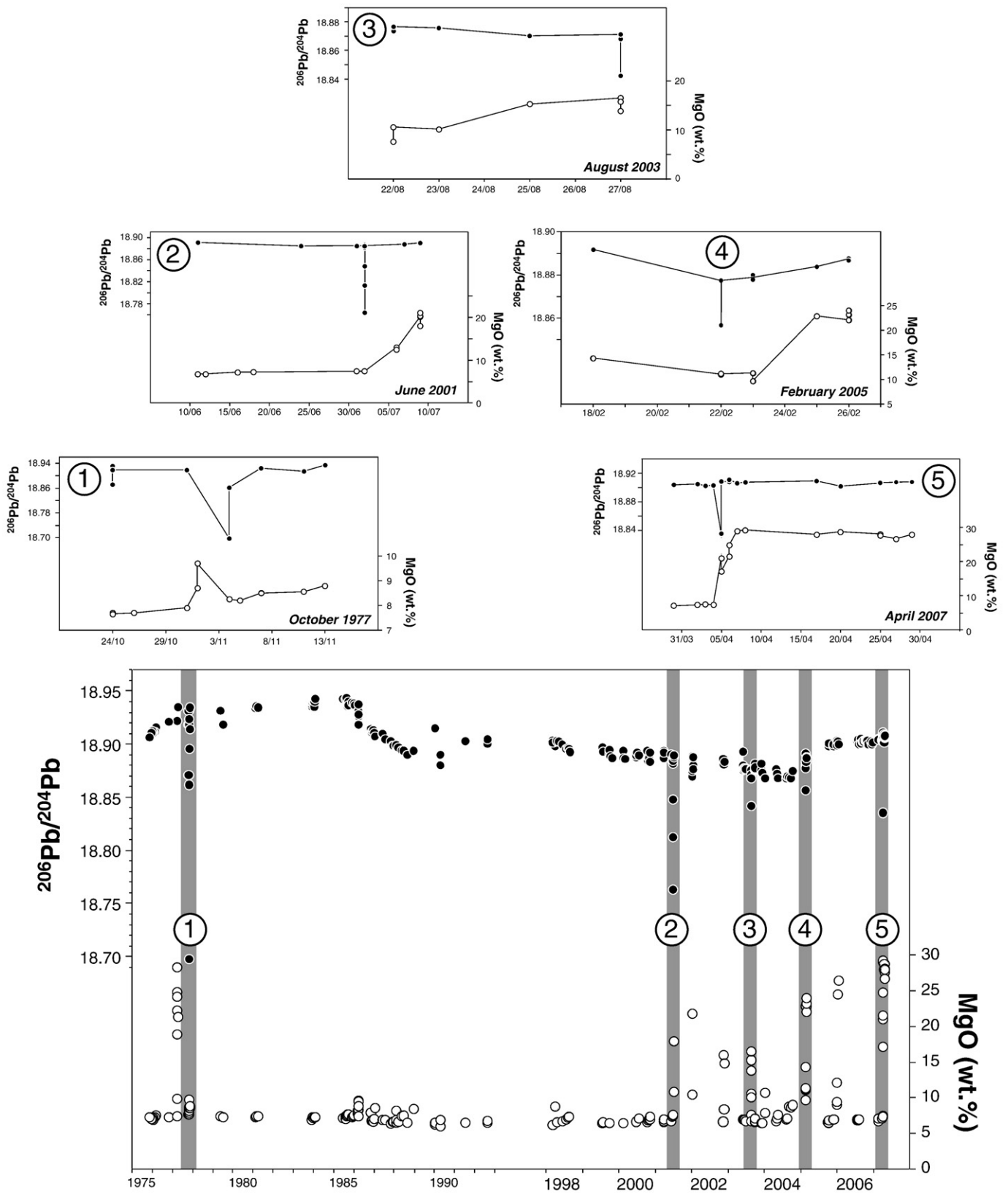


Fig. 5. Relations between Pb unradiogenic anomalies and eruptions of olivine-rich lavas. Unradiogenic Pb spikes coincide with basalt-oceanite transition (April 2007), or occur a few days before (July 2001, February 2005) or after (August 2003) such transitions. In 1977, the unradiogenic anomaly occurred a few months after the April oceanite eruption.

2005, 2007 and this work) are plotted versus time together with previously published data on historical samples (Fig. 8). Strontium isotopic variations are small, but nevertheless larger than analytical error. From 1927 to ~1985, published data seem to define a trend of

increasing $^{87}\text{Sr}/^{86}\text{Sr}$. Subsequently, from 1986 to 1992, our data document a rapid decrease of $^{87}\text{Sr}/^{86}\text{Sr}$. The beginning of the 1998 eruptive cycle is characterized by a heterogeneous Sr isotope signature. The main vent (Kapor) produced lavas with unradiogenic

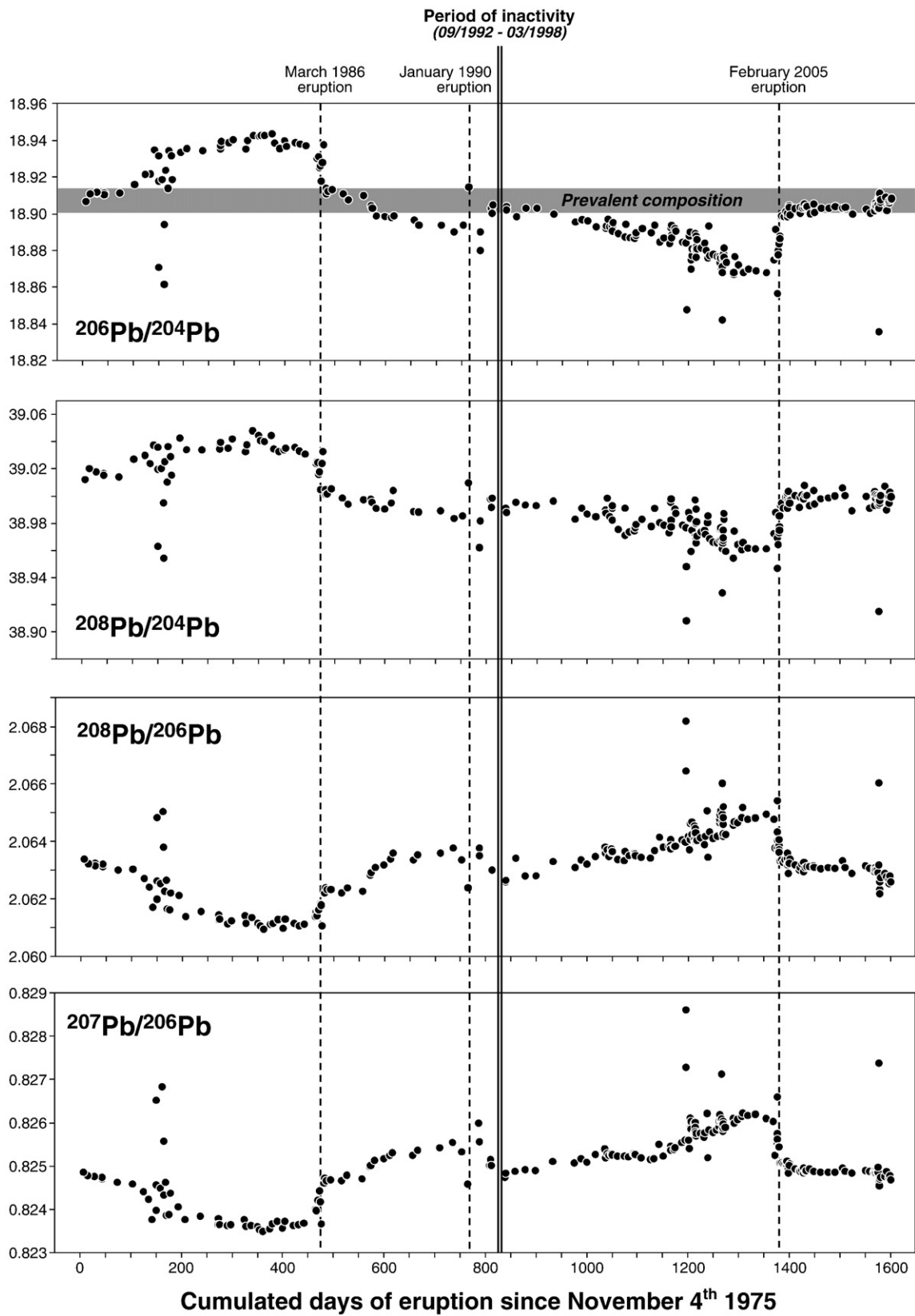


Fig. 6. Lead isotopic compositions plotted against cumulated days of eruption since November 4th 1975. Data are from Table 1 and Vlastélic et al. (2005, 2007).

Sr signature ($^{87}\text{Sr}/^{86}\text{Sr} = 0.704104$), as in 1992, whereas the separate vent (Hudson), which was briefly active in March 1998, shows a more radiogenic signature ($^{87}\text{Sr}/^{86}\text{Sr} = 0.704245$), resembling those from the 1975–1985 period. Then, from 2001 to 2006, Sr isotopic

compositions are remarkably uniform ($^{87}\text{Sr}/^{86}\text{Sr} \sim 0.70418$) and similar to the average composition of historical lavas. Variations of Nd isotope compositions ($3.96 < \epsilon_{\text{Nd}} < 4.35$) are barely outside analytical error ($\sim 0.16 \epsilon_{\text{Nd}}$). However, the negative relationship between

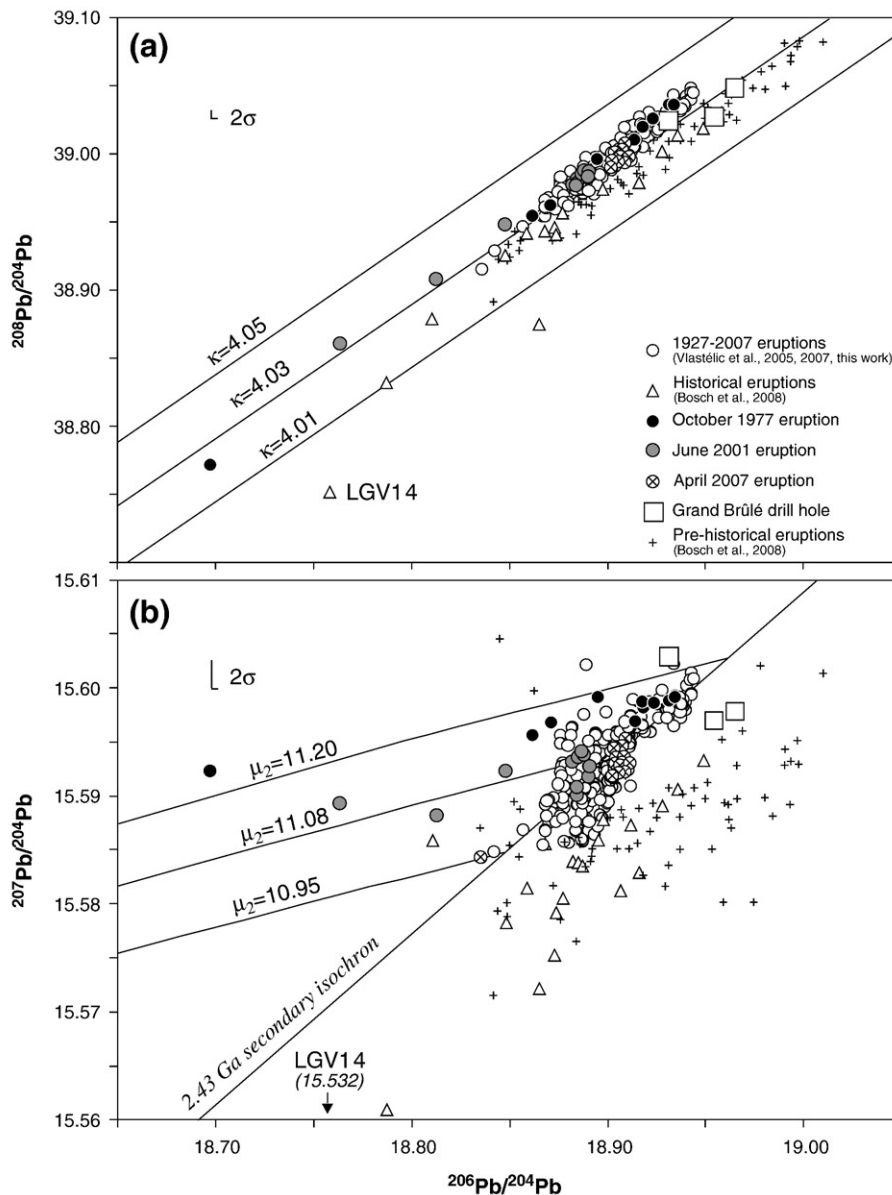


Fig. 7. Lead–lead isotope relationships in Piton de la Fournaise lavas. Data are from Table 1 and Vlastélic et al. (2005, 2007). Renormalized data from Bosch et al. (2008), including those from pre-historical eruptions, are also shown. The slight offset between our data and those from Bosch et al. (2008) could reflect a slight difference in mass fractionation correction and/or imperfect renormalization of Bosch et al. (2008) data. (a) $^{208}\text{Pb}/^{204}\text{Pb}$ vs. $^{206}\text{Pb}/^{204}\text{Pb}$ plot. Each line indicates the composition the primordial material would have today if it evolved in closed system with respect to $^{232}\text{Th}/^{238}\text{U}$ (κ) since 4.56 Ga. (b) $^{207}\text{Pb}/^{204}\text{Pb}$ vs. $^{206}\text{Pb}/^{204}\text{Pb}$ plot. Our data (Vlastélic et al., 2005, 2007, this work) plot along a 2.43 Ga secondary isochron. Assuming this age is that of $^{238}\text{U}/^{204}\text{Pb}$ increase, the Pb isotopic variations can be modeled in a two-stage history, with $\mu_1 = 7.93$ and μ_2 ranging from 10.95 to 11.20. Isotopic growth curves are shown for different values of μ_2 .

Nd and Sr isotopes (Fig. 8) supports the existence of tiny, but real, $^{143}\text{Nd}/^{144}\text{Nd}$ variations (in particular between 1977 and 1998). Only rare co-variations are observed between Sr, Nd and Pb isotopes. Between 1985 and 1988, both Pb and Sr ratios decrease whereas Nd ratios slightly increase. However, considering the whole data set, neither Sr nor Nd isotopes correlate with Pb isotopes. In particular, samples showing unradiogenic Pb anomalies (erupted in October 1977 and July 2001) display normal Sr and Nd isotopic compositions.

6. Discussion

6.1. Decoupling of Pb from Sr and Nd isotopes

A first key observation is that Pb isotopes are decoupled from Sr and Nd isotopes, which show small variations in historical lavas from Piton de la Fournaise. In addition, the co-variations of $^{206}\text{Pb}/^{204}\text{Pb}$ and $^{208}\text{Pb}/$

^{204}Pb at nearly constant $(^{208}\text{Pb})^*/(^{206}\text{Pb})^*$ (Fig. 7a) indicate that coupled $^{238}\text{U}/^{204}\text{Pb}$ and $^{232}\text{Th}/^{204}\text{Pb}$ fractionation occurred with very small $^{232}\text{Th}/^{238}\text{U}$ fractionation. The fact that only time-integrated ratios involving Pb display significant variations points out an anomalous behavior of Pb in the Réunion plume source. The affinity of Pb for sulfides is generally invoked to account for the anomalous behavior of Pb in the mantle (Hart and Gaetani, 2006).

Short-term variations of Pb isotopes at Piton de la Fournaise could reflect shallow-level processes, such as wall-rock interactions or, alternatively, long-lived heterogeneities within the Réunion plume source. None of these hypotheses can be firmly ruled out on the basis of the new observations. To date, historical, coupled Pb–Sr–Nd variations at Hawaiian active volcanoes have been ascribed to small-scale heterogeneity of the plume (Pietruszka and Garcia, 1999a; Marske et al., 2007). At Piton de la Fournaise, the relatively large Pb isotopic variations at nearly constant Nd isotope composition, and the existence of a close

Table 2
Sr and Nd isotopic compositions of 17 selected samples (1977–2006).

Sample name	Eruption date	$^{87}\text{Sr}/^{86}\text{Sr}$	$^{143}\text{Nd}/^{144}\text{Nd}$	ϵ_{Nd}	Dissolution
77-14 dup	1977/11/4	0.704214	0.512844	4.02	r*
77-14 ter		0.704216	0.512847	4.08	r*
858-281	1985/8/28	0.704189	0.512850	4.14	r*
863-281	1986/3/28	0.704179	0.512853	4.19	r
885-1	1988/5/18	0.704164	0.512855	4.23	r
928-28	1992/8/28	0.704100	0.512861	4.35	r
989-036 (Kapor)	1998/3/10	0.704104	0.512853	4.19	p
986-115 (Hudson)	1998/3/30	0.704245	0.512846	4.06	p
0106-111	2001/6/11	0.704182	0.512842	3.98	p
0107-022	2001/7/2	0.704174	0.512845	4.04	p
0107-022 dup		0.704172	0.512843	4.00	p
0201-143	2002/1/14	0.704173	0.512846	4.06	p
0308-275	2003/8/27	0.704170	0.512856	4.25	p
0408-132	2004/8/13	0.704175	0.512861	4.35	p
0502-221	2005/2/22	0.704181	0.512855	4.23	p
0502-263	2005/2/26	0.704182	0.512847	4.08	p
0601-181	2006/1/18	0.704173	0.512853	4.19	p
0607-281	2006/7/28	0.704177	0.512841	3.96	p
0608-021	2006/8/2	0.704166	0.512858	4.29	p

Sr compositions are relative to $^{87}\text{Sr}/^{86}\text{Sr} = 0.710243 \pm 9$ (2σ) for NBS 987 standard.
Nd compositions are relative to $^{143}\text{Nd}/^{144}\text{Nd} = 0.511958 \pm 8$ (2σ) for AMES Rennes standard.
p: powder; r: rock chip.

*same dissolution as for Pb isotopes (Table 1).

dup: duplicate dissolution; ter: triplicate dissolution.

Corresponding Pb isotopic compositions are given in Table 1 and in Vlastélic et al. (2005, 2007).

relationship between unradiogenic Pb anomalies and eruptions of olivine-rich lavas, rather suggest that shallow-level processes dominantly control the Pb isotopic signal. Such a difference in the message carried by Pb isotopes at these two volcanoes could reflect fundamental differences between the two associated major plumes. At Hawaii, lava production rate is one order of magnitude higher than at Réunion. As the voluminous feeding system of Kilauea volcano has a simple shape, plume heterogeneities may be preserved in the erupted lavas (Pietruszka and Garcia, 1999b). On the basis of the volume of magma produced ($\sim 1 \text{ km}^3$), the 1927–2007 activity of Piton de la Fournaise can be compared to the first 13 years (1983–1995) of the Puu Oo eruption of Kilauea. Then, the isotopic variations at Kilauea – Pb ($\Delta^{206}\text{Pb}/^{204}\text{Pb} \sim 0.14$) > Sr ($\Delta^{87}\text{Sr}/^{86}\text{Sr} \sim 0.00006$) > Nd (within analytical error) (Garcia et al., 1996) –, which were ascribed to mixing primitive plume melts with an evolved rift zone magma during the first two years of eruption, are similar to those identified at Piton de la Fournaise and, similarly, point Pb isotopes as a particularly sensitive tracer of shallow-level processes.

Hart and Gaetani (2006) who investigated the distinctive behavior of sulfides in the mantle and the implications for Pb, explained how and why the Pb isotopic signature of plume melts might be modified at shallow level. Plume material stripped of its S near the sulfide solidus tends to assimilate or equilibrate with genetically unrelated sulfides from the lithosphere or the crust. This process is enhanced at shallower levels as the solubility of sulfides in silicate melts increases with decreasing pressure. Indeed, the identification of sulfide globules in olivine and olivine-hosted melt inclusions from Piton de la Fournaise (Bureau et al., 1998) indicates that melts are saturated in S. Fast diffusion of Pb in sulfides and the possible existence of sulfide melt network also raise the possibility that Pb exchange between plume melts and crustal rocks is faster than for lithophile elements. In addition to the points raised by Hart and Gaetani (2006), it can also be argued that the relatively low melting temperature of sulfides could lead to their preferential dissolution when hot ascending magmas interact with colder wall-rocks.

6.2. Unradiogenic Pb anomalies

There is growing evidence for the existence of rare but pronounced unradiogenic Pb compositions in Piton de la Fournaise lavas. Six par-

ticularly unradiogenic compositions ($^{206}\text{Pb}/^{204}\text{Pb} < 18.83$, see Fig. 4) have been reported in samples from 1931, 1945, 1977 and 2001 (Vlastélic et al., 2005; Bosch et al., 2008; this work), the most extreme composition ($^{206}\text{Pb}/^{204}\text{Pb} = 18.6972$) being encountered in a leached sample from 1977. In addition, Bosch et al. (2008) reported particularly low $^{207}\text{Pb}/^{204}\text{Pb}$ and $^{208}\text{Pb}/^{204}\text{Pb}$ (15.532 and 38.753, respectively) and moderately low $^{206}\text{Pb}/^{204}\text{Pb}$ (18.761) in an ankaramite from Rivière Langevin (50 to 70 ka old). These unradiogenic Pb compositions were ascribed to the interaction of lavas with hydrothermally altered basalts or cumulates from the volcanic edifice or the underlying crust, although such explanation did not account for the absence of Sr and Nd isotopic anomalies in the related samples.

It is evident from Fig. 7 that a single unradiogenic component cannot account for the various unradiogenic Pb compositions. For instance, the low $^{207}\text{Pb}/^{204}\text{Pb}$ and $^{208}\text{Pb}/^{204}\text{Pb}$ ratios of the ankaramite (LGV 14) could reflect assimilation of the Indian oceanic crust on which the volcano rests. On the other hand, the anomalous samples from 1977 and 2001 are characterized by low $^{206}\text{Pb}/^{204}\text{Pb}$ and $^{208}\text{Pb}/^{204}\text{Pb}$ but normal $^{207}\text{Pb}/^{204}\text{Pb}$. These samples carry a distinctive unradiogenic component, which cannot be the underlying oceanic crust (which is expected to have lower $^{207}\text{Pb}/^{204}\text{Pb}$ than Réunion plume melts).

In $^{207}\text{Pb}/^{204}\text{Pb}$ vs. $^{206}\text{Pb}/^{204}\text{Pb}$ space, samples from October 1977 eruption define a sub-horizontal array suggesting a recent modification of their U/Pb. Simple modeling of Pb isotopic growth curves suggests that the unradiogenic compositions result from freezing Pb isotopic evolution less than 160 Ma ago, perhaps by incorporation of Pb in sulfides. Alternatively, the array may reflect mixing between plume melts and a contaminant having similar $^{207}\text{Pb}/^{204}\text{Pb}$ but lower $^{206}\text{Pb}/^{204}\text{Pb}$ and $^{208}\text{Pb}/^{204}\text{Pb}$. The lack of reproducibility of the replicate analyses of the most anomalous samples (November 4th 1977 and July 2nd 2001) suggests that samples are heterogeneous at a sub-millimeter scale. In addition, leaching experiments performed on samples from July 2nd 2001 indicate that unradiogenic Pb resides in a phase that is not dissolved during strong leaching. It is possible that this phase is olivine-hosted melt inclusions, which have been shown to contain highly heterogeneous and unradiogenic Pb (Saal et al., 2005). This would explain the close relationship between unradiogenic Pb anomalies and eruptions of olivine-rich lavas. Saal et al. (2005) suggested that Pb isotopic signature of melt inclusions records interactions between plume melts and the lithosphere through which they percolated. Vlastélic et al. (2007) proposed that the most unradiogenic compositions could reflect assimilation of Pb-rich hydrothermal deposits lying on top of the oceanic crust. Although the exact depth of contamination and the nature of the contaminant remain poorly constrained, the absence of unradiogenic material within the volcanic edifice (as suggested by the study of old lavas and gabbroic cumulates recovered from the Grand Brûlé drill hole) implies that the unradiogenic Pb signature must be acquired at the oceanic crustal level or even deeper. The relationship between unradiogenic Pb compositions and high-flux eruption of olivine-rich lavas has been explained in a model where deep magma storage controls both assimilation and effusion rate (Vlastélic et al., 2005). The relatively primitive composition of cumulative olivine (Fo_{84} against Fo_{80} in olivine phenocrysts) subsequently supported the idea that oceanites segregate from great depths to lavas from summit eruptions (Peltier et al., 2006). In most cases, unradiogenic Pb compositions coincide with transitions from basalt to oceanite. The voluminous, densely sampled eruption of April 2007, which offers a detailed view of a basalt-oceanite transition, clearly shows that the isotopic anomaly is only present in the first sample containing cumulative olivine, and that the oceanites erupted after the transition have the same composition as the early erupted basalts (Fig. 5). One possible explanation is that the pulse of magma that disrupted olivine cumulates cleaned the magma conduit. Such a magma pulse could also have entrained dense, Pb-rich sulfides that are expected to pond near the

sulfide solidus (Hart and Gaetani, 2006). However, the connection between unradiogenic spikes and occurrence of cumulative olivine is not always as clear as in April 2007 (Fig. 5). Further investigations of

the anomalous samples, such as mapping the distribution of Pb isotopes at the crystal scale, are needed to better constrain the processes by which oceanites form.

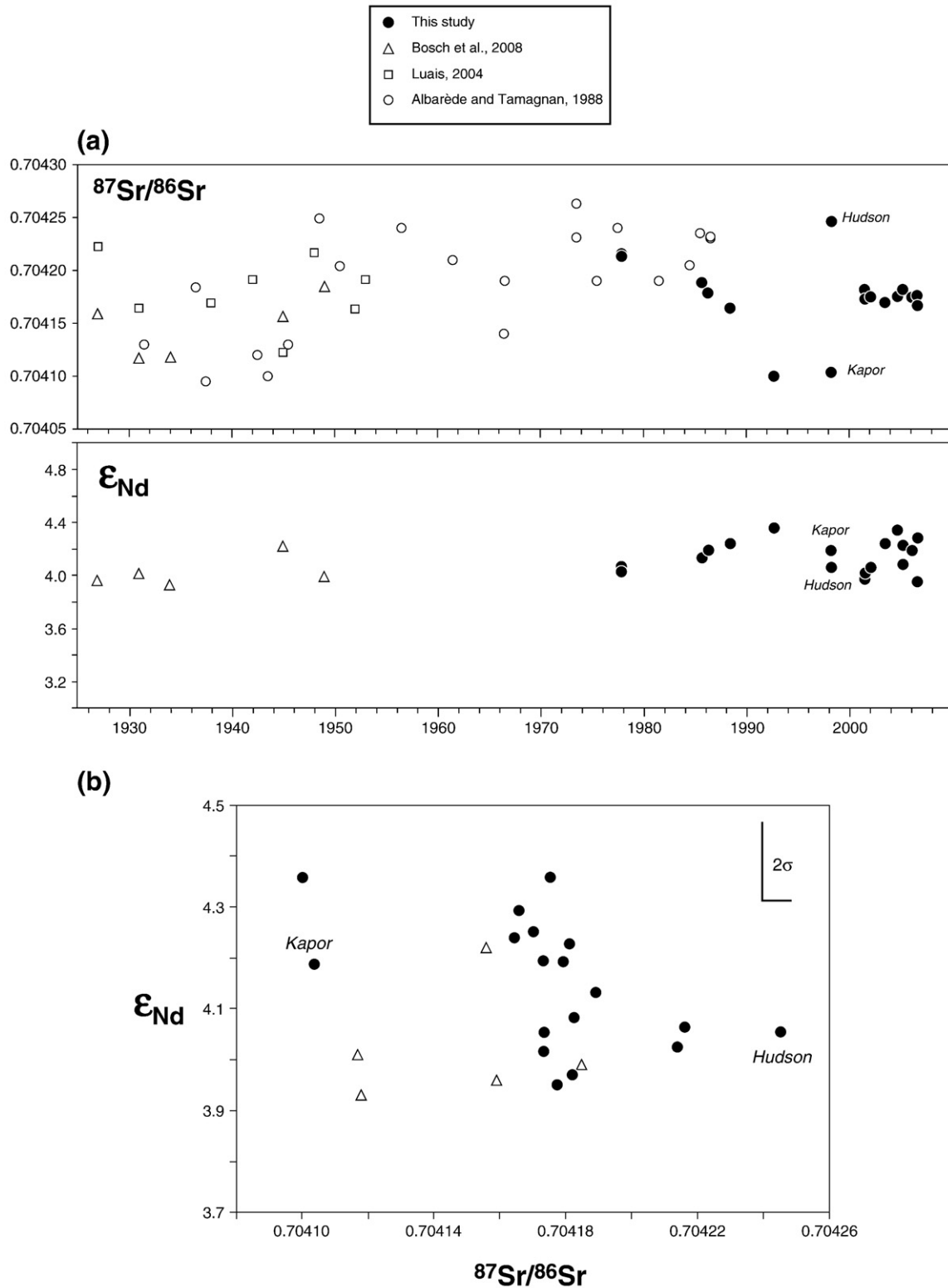


Fig. 8. Sr and Nd isotope systematics of Piton de la Fournaise historical lavas. (a) Sr and Nd isotopes versus time. (b) Sr–Nd isotope relationships. Data are from Table 2, Albarède and Tamagnan (1988), Luais (2004) and Bosch et al. (2008). Sr data from Luais (2004) and Bosch et al. (2008) have been re-normalized to $^{87}\text{Sr}/^{86}\text{Sr} = 0.710243$ for the NBS 987 standard, whereas Nd data were not re-normalized (in the absence of precise cross-calibration of the different Nd isotopic standards). Nd data acquired by MC-ICPMS (Luais, 2004) are not shown because they plot above TIMS data. However, these MC-ICPMS Nd data broadly overlap with TIMS data (within a range of $+4.04$ to $+4.72 \pm 0.24(2s)$) when renormalized to the identical standard value (B. Luais, personal communication, 2008).

6.3. Temporal variation of Pb isotopes

The recent decrease of $^{206}\text{Pb}/^{204}\text{Pb}$ in Piton de la Fournaise lavas, from 18.90 in 1998 to 18.87 in 2004, has been modeled as resulting from injection of an homogenous batch of plume melts (with $^{206}\text{Pb}/^{204}\text{Pb} = 18.90$) within a dyke system followed by depth-dependent crustal contamination, the late-erupting lavas stored at the oceanic crust level being the most contaminated (Vlastélic et al., 2007). The sudden return of $^{206}\text{Pb}/^{204}\text{Pb}$ to ~ 18.90 in 2005 was interpreted as refilling the plumbing system with deep, uncontaminated plume melts.

At the century scale, the prevalent composition (see section 5.1), which defines some kind of baseline, supports the hypothesis that plume melts have $^{206}\text{Pb}/^{204}\text{Pb}$ close to 18.90, as previously assumed in the study of most recent eruptions. Many historical eruptions, and in particular those from the 1977–1985 period, display Pb isotopic compositions that are more radiogenic than this assumed plume composition, however. Such radiogenic compositions ($^{206}\text{Pb}/^{204}\text{Pb}$ up to 18.9437) require interactions with a radiogenic contaminant, which could be the old lava flows making the deep layers of the volcanic edifice (Bosch et al. (2008) reported $^{206}\text{Pb}/^{204}\text{Pb}$ up to 19.075 for Piton des Neiges lavas). The small isotopic difference between plume melts and contaminant would require extensive assimilation, however. For instance, assuming identical Pb content between plume and contaminant (both being Réunion lavas), assimilation rates would be 25% to 45% (with $^{206}\text{Pb}/^{204}\text{Pb}$ of the contaminant ranging from 19.075 to 19.000). Partial melting of the contaminant would lower these estimates and thus make assimilation a more realistic scenario. If this interpretation is correct, one may wonder why melt would assimilate shallow edifice material between 1977 and 1986 and deep crustal material between 1998 and 2004. One explanation, inspired from the model proposed to account for 1998–2004 unradiogenic signature (Vlastélic et al., 2007), would be that a major injection of homogeneous plume melts occurred prior 1975, filling the whole plumbing system. If depth-dependent contamination is effective, the 1975–2005 isotopic variations could thus reflect progressive emptying of the storage system. As previously pointed out, such scenario requires long period of storage followed by rapid transfer of magmas

from their storage location to the surface. The hypothetical major injection could have occurred between 1966 and 1972, which is the longest known period of quiescence since the beginning of the 20th century. Another possibility is that the release of latent heat of crystallization controls partial melting of the surrounding rocks (Spera and Bohrsen, 2001). Hence, difference in assimilation level between 1977–1986 and 1998–2004 periods may reflect differences in crystallization depths of magmas.

6.4. Implications for magma storage and transfer

As previously observed for the most recent period, Pb isotopic variations occurred essentially during eruptions and not between. Supporting this observation, Pb isotopic composition did not evolve significantly during the longest periods of quiescence (>3 years) whose delimiting eruptions have been studied (1939–1942, 1966–1972, 1992–1998) (Fig. 4). The 1992–1998 period of quietness is by far the best documented based on both geochemical and geophysical data. Two vents were simultaneously active at the beginning of the 1998 eruptive cycle. Pre-eruptive migration of earthquakes suggested that magmas feeding the major long-lived vent (Kapor) segregated from a reservoir located at about 5 km below sea level (b.s.l.) (Battaglia et al., 2005). On the other hand, several observations (Bureau et al., 1999; Semet et al., 2003) indicated that the lavas erupted at the smaller, remote vent (Hudson) segregated rapidly from lithospheric mantle depths (about 15 km b.s.l.). The first lavas erupted at Kapor vent have similar Pb, Sr and Nd isotopic compositions, and also K content (Boivin and Bachèlery, 2009–this issue) as the last lavas erupted in 1992. In contrast, Hudson lavas exhibit distinctively higher $^{87}\text{Sr}/^{86}\text{Sr}$ and K content, lower $^{143}\text{Nd}/^{144}\text{Nd}$ but similar Pb isotope signature. Isotopic data support the idea that 1998 Kapor lavas and 1992 lavas sampled the same magma reservoir located near the bottom of the volcanic edifice, whereas Hudson vent sampled uncontaminated plume melts, which bypassed the central feeding system. The Pb isotopic drift seen during the six months long activity of the Kapor vent does not support the existence of an homogeneous reservoir, but rather suggests progressive emptying of a vertically zoned magma

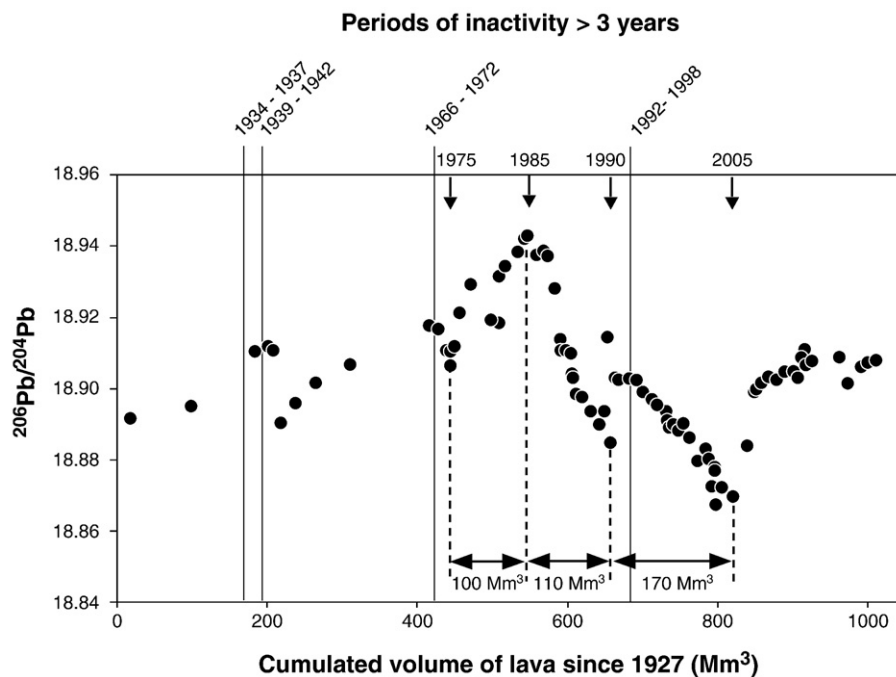


Fig. 9. $^{206}\text{Pb}/^{204}\text{Pb}$ versus volume of lava erupted since 1927. The longest periods of inactivity (>3 years) as well as eruptions bracketing isotopic gradients are indicated. For each eruption, the average Pb isotope composition is plotted versus half erupted volume. Exceptions are the voluminous, densely sampled eruptions of March 1998 and April 2007, for which we report individual data points assuming constant effusion rates.

conduit, whose deepest products would have interacted with the oceanic crust.

The absence of Pb isotopic variations during long periods of inactivity indicates that lavas can be stored for years without being contaminated. At first glance, this observation questions the idea that wall-rock interactions dominantly control the Pb isotopic signal. Plotting Pb isotopes against cumulated volume of magma (Fig. 9) indicates that the volume of magma presumably contaminated is relatively small. For instance, on the ~1000 Mm³ of magma erupted between 1927 and 2007, about 750 Mm³ have 18.89 ²⁰⁶Pb/²⁰⁴Pb < 18.91. Intermediate compositions also bracket the longest inactive periods (²⁰⁶Pb/²⁰⁴Pb = 18.911, 18.917 and 18.904 for 1939–1942, 1966–1972 and 1992–1998 quiet periods, respectively). These observations support the existence of a magma reservoir that is sufficiently voluminous to prevent extensive contamination and buffer Pb isotopic composition. More or less direct sampling of this reservoir would account for the small Pb isotopic variability in ~3/4 of the volume of magma erupted since 1927. Alternatively, such an intermediate, highly frequent composition may reflect direct sampling of plume melts. Isotopic gradients (1975–1985, 1986–1990, 1998–2004), which systematically diverged from this prevalent composition, may reflect progressive emptying of smaller magma reservoirs or magma conduits, which are expected to be more sensitive to wall-rock interactions than the main magma chamber. These temporal gradients, observed through volumes of magmas ranging from ~100 Mm³ to ~170 Mm³ (Fig. 9), provide lower bounds for the size of the shallow magma storage system. Rapid isotopic shifts occurring at the eruption scale (March 1986, January–April 1990, February 2005) systematically converged towards the prevalent composition. They are best modeled as resulting from mixing magmas already residing in the shallow plumbing system (sampled by previous eruptions) with newly injected, deeper magmas. The volume of lava erupted between the major refilling events of March 1986 and February 2005 (280 Mm³) could reflect the size of the magma reservoir of Piton de la Fournaise.

7. Conclusion

Over the last 20 years, both uranium series disequilibria (Condomines et al., 1988; Sigmarsson et al., 2005) and short-term fluctuations of radiogenic isotopes and trace element ratios (Albarède and Tamagnan, 1988; Albarède, 1993) have been used to constrain magma chamber dynamics beneath Piton de la Fournaise. The second approach, which is based on the resolution of small compositional changes, has recently gained from the possibility of measuring highly precise isotopic compositions on new generation mass spectrometers. Here, we used a Nu MC-ICPMS to resolve fine Pb isotopic changes in the most recent eruptions of Piton de la Fournaise. The main findings are summarized below.

Historical lavas (1927–2007) from Piton de la Fournaise display Pb isotopic variations, which are both large (about 80% of the total variations observed for the volcano) and systematic. The decoupling of Pb from Sr and Nd isotopes, which display small and barely significant variations, respectively, points out the chalcophilic behavior of Pb as the main cause of the fluctuations of its isotopic composition. Although the possibility that the rapid Pb isotopic variations reflect small-scale zoning of the Réunion plume cannot be definitely ruled out, several considerations of the expected behavior of sulfides during melting and magma segregation suggest that the Pb isotopic signal has a shallow origin. Assuming that Pb isotopic variations reflect wall-rock interactions occurring at different levels, it is possible to distinguish periods of eruption of stale magmas from those of refilling the plumbing system with pristine plume melts. Fluctuations of Pb isotopes in the recent, densely sampled eruptions (1975–2007) provide a lower bound (0.1 to 0.17 km³) and a best estimate (0.28 km³) for the size of the shallow storage system of Piton de la Fournaise volcano. Such volumes agree with previous estimates based on geochemical data (0.1 to 0.35 km³) (Albarède, 1993; Sigmarsson et al., 2005). Unradiogenic spikes (²⁰⁶Pb/

²⁰⁴Pb down to 18.6972) appear to be linked to the occurrence of olivine-rich lavas. A better knowledge of the distribution of Pb isotopes within some of these samples, which are isotopically heterogeneous at the sub-millimeter scale, would certainly improve our understanding of the origin of Piton de la Fournaise oceanites.

Acknowledgements

Thanks to F. Albarède for the helpful comments and to an anonymous reviewer for giving his opinion. M. Bésairie, K. David and J.L. Piro (LMV, Clermont-Ferrand) provided technical assistance in the lab. The authors are grateful to L. Michon for handling the manuscript. This study benefited from the financial support of ACI/FNS program “Aléas et changements globaux”.

References

- Albarède, F., 1993. Residence time analysis of geochemical fluctuations in volcanic series. *Geochimica et Cosmochimica Acta* 57, 615–621.
- Albarède, F., Tamagnan, V., 1988. Modelling the recent geochemical evolution of the Piton de la Fournaise volcano, Réunion island, 1931–1986. *Journal of Petrology* 29, 997–1030.
- Albarède, F., Luais, B., Fitton, G., Semet, M., Kaminski, E., Upton, B.G.J., Bachèlery, P., Cheminée, J.L., 1997. The geochemical regimes of Piton de la Fournaise volcano (Réunion) during the last 530 000 years. *Journal of Petrology* 38, 171–201.
- Bachèlery, P., 1981. Le Piton de la Fournaise (Ile de la Réunion). Etude volcanologique, structurale et pétrologique. Thèse, Université de Clermont-Ferrand, France.
- Battaglia, J., Ferrazzini, V., Staudacher, T., Aki, K., Cheminée, J.-L., 2005. Pre-eruptive migration of earthquakes at the Piton de la Fournaise volcano (Réunion Island). *Geophysical Journal International* 161, 549–558.
- Boivin, P., Bachèlery, P., 2009. Petrology of 1977 to 1998 eruptions of Piton de la Fournaise, La Réunion Island. *Journal of Volcanology and Geothermal Research* 184, 109–125 (this issue).
- Bosch, D., Blichert-Toft, J., Moynier, F., Nelson, B.K., Télouk, P., Gillot, P.-Y., Albarède, F., 2008. Pb, Hf and Nd isotope compositions of the two Réunion volcanoes (Indian Ocean): A tale of two small-scale mantle “blobs”? *Earth and Planetary Science Letters* 265, 748–768.
- Bureau, H., Pineau, F., Métrich, N., Semet, M., Javoy, M., 1998. A melt and fluid inclusion study of the gas phase at Piton de la Fournaise volcano (Réunion Island). *Chemical Geology* 147, 115–130.
- Bureau, H., Métrich, N., Semet, M., Staudacher, T., 1999. Fluid-magma decoupling in a hot-spot volcano. *Geophysical Research Letters* 23, 3501–3504.
- Condomines, M., Hémond, C., Allègre, C.J., 1988. U–Th–Ra radioactive disequilibria and magmatic processes. *Earth and Planetary Science Letters* 90, 243–262.
- Fisk, M.R., Upton, B.G.J., White, W.M., 1988. Geochemical and experimental study of the genesis of magmas of Réunion Island, Indian Ocean. *Journal of Geophysical Research* 93, 4933–4950.
- Fretzdorff, S., Haase, K.M., 2002. Geochemistry and petrology of lavas from the submarine flanks of Réunion Island (western Indian Ocean): implications for magma genesis and mantle source. *Mineralogy and Petrology* 75, 153–184.
- Garcia, M.O., Rhodes, J.M., Trusdell, F.A., Pietruszka, A.J., 1996. Petrology of lavas from the Puu Oo eruption of Kilauea volcano: III. The Kupaianaha episode (1986–1992). *Bulletin of Volcanology* 58, 359–379.
- Graham, D., Lupton, J., Albarède, F., Condomines, M., 1990. Extreme temporal homogeneity of helium isotopes at Piton de la Fournaise, Réunion Island. *Nature* 347, 545–548.
- Hart, S., Gaetani, G.A., 2006. Mantle Pb paradoxes: the sulfide solution. *Contributions to Mineralogy and Petrology* 152, 295–308.
- Lénat, J.-F., Gibert-Malengreau, B., 2001. A new model for the evolution of the volcanic island of Réunion (Indian Ocean). *Journal of Geophysical Research* 106, 8645–8663.
- Lénat, J.-F., Bachèlery, P., Bonneville, A., Hirn, A., 1989. The beginning of the 1985–1987 eruptive cycle at Piton de la Fournaise (La Réunion); new insights in the magmatic and volcano-tectonic systems. *Journal of Volcanology and Geothermal Research* 36, 209–232.
- Luais, B., 2004. Temporal changes in Nd isotopic composition of Piton de la Fournaise magmatism (Réunion Island, Indian Ocean). *Geochemistry Geophysics Geosystems* 5, Q01008. doi:10.1029/2002GC000502.
- Lugmair, G.W., Galer, S.J.G., 1992. Age and isotopic relationships among the angrites Lewis Cliff 86010 and Angra dos Reis. *Geochimica et Cosmochimica Acta* 56, 1673–1694.
- Marske, J.P., Pietruszka, A.J., Weis, D., Garcia, M.O., Rhodes, J.M., 2007. Rapid passage of a small-scale mantle heterogeneity through the melting regions of Kilauea and Mauna Loa Volcanoes. *Earth and Planetary Science Letters* 259, 34–50.
- Michon, L., Staudacher, T., Ferrazzini, V., Bachèlery, P., Marti, J., 2007. April 2007 collapse of Piton de la Fournaise: a new example of caldera formation. *Geophysical Research Letters* 34, L21301. doi:10.1029/2007GL031248.
- Oversby, V.M., 1972. Genetic relations among the volcanic rocks of Réunion: chemical and lead isotopic evidence. *Geochimica et Cosmochimica Acta* 36, 1167–1179.
- Peltier, A., Bachèlery, P., Semet, M., Staudacher, T., 2006. Geophysical and geochemical arguments for three levels of dyke initiations in the shallower reservoir at Piton de la Fournaise volcano. *Eos Trans. AGU*, 87(52), Fall Meet. Suppl., Abstract V24A-05.

- Pietruszka, A.J., Garcia, M.O., 1999a. A rapid fluctuation in the mantle source and melting history of Kilauea volcano inferred from the geochemistry of its historical summit lavas (1790–1982). *Journal of Petrology* 40, 1321–1342.
- Pietruszka, A.J., Garcia, M.O., 1999b. The size and shape of Kilauea Volcano's summit magma storage reservoir: a geochemical probe. *Earth and Planetary Science Letters* 167, 311–320.
- Pin, C., Zalduégui, J.F.S., 1997. Sequential separation of light rare-earth elements, thorium and uranium by miniaturized extraction chromatography: application to isotopic analyses of silicate rocks. *Analytica Chimica Acta* 339, 79–89.
- Pin, C., Briot, D., Bassin, Ch., Poitrasson, F., 1994. Concomitant separation of strontium and samarium-neodymium for isotopic analysis in silicate samples, based on specific extraction chromatography. *Analytica Chimica Acta* 298, 209–217.
- Rançon, J.P., Lerebour, P., Augé, T., 1989. The Grand Brûlé exploration drilling: new data on the deep framework of the Piton de la Fournaise volcano. Part 1: Lithostratigraphic units and volcanostructural implications. *Journal of Volcanology and Geothermal Research* 36, 113–127.
- Saal, A.E., Hart, S.R., Shimizu, N., Hauri, E.H., Layne, G.D., Eiler, J.M., 2005. Pb isotopic variability in melt inclusions from the EM1–EMII–HIMU mantle end-members and the role of the oceanic lithosphere. *Earth and Planetary Science Letters* 240, 605–620.
- Semet, M.P., Joron, J.-L., Staudacher, T., 2003. The 1998–2002 activity of Piton de la Fournaise, Réunion Island: lessons in magma supply and transfers. *Geophysical Research Abstracts* 5, 10736.
- Sigmarsson, O., Condomines, M., Bachèlery, P., 2005. Magma residence time beneath the Piton de la Fournaise volcano, Réunion Island, from U-series disequilibria. *Earth and Planetary Science Letters* 234, 223–234.
- Spera, F.J., Bohrsen, W.A., 2001. Energy-constrained open-system magmatic processes. I: general model and energy-constrained assimilation and fractional crystallization (EC-AFC) formulation. *Journal of Petrology* 42, 999–1018.
- Staudacher, T., Sarda, P.S., Allègre, C.J., 1990. Noble gas systematics of Réunion island, Indian Ocean. *Chemical Geology* 89, 1–17.
- Staudacher, T., Ferrazzini, V., Peltier, A., Kowalski, P., Boissier, P., Catherine, P., Lauret, F., Massin, F., 2009. The April 2007 eruption and the Dolomieu crater collapse, two major events at Piton de la Fournaise (La Réunion Island, Indian Ocean). *Journal of Volcanology and Geothermal Research* 184, 126–137 (this issue).
- Stieltjes, L., Moutou, P., 1989. A statistical and probabilistic study of the historic activity of Piton de la Fournaise, Réunion Island, Indian Ocean. *Journal of Volcanology and Geothermal Research* 36, 67–86.
- Vlastélic, I., Staudacher, T., Semet, M., 2005. Rapid change of lava composition from 1998 to 2002 at Piton de la Fournaise (Réunion) inferred from Pb isotopes and trace elements: evidence for variable crustal contamination. *Journal of Petrology* 46, 79–107.
- Vlastélic, I., Peltier, A., Staudacher, T., 2007. Short-term (1998–2006) fluctuations of Pb isotopes at Piton de la Fournaise volcano (Réunion Island): origins and constraints on the size and shape of the magma reservoir. *Chemical Geology* 244, 202–220.
- White, W.M., Albarède, F., Télouk, P., 2000. High-precision analysis of Pb isotopic ratios by multi-collector ICP-MS. *Chemical Geology* 167, 257–270.